New Model for the High Modulus and Strength Performance of Ultradrawn Polyethylenes

ANAGNOSTIS E. ZACHARIADES, *IBM Research Division, Almaden Research Center, 650 Harry Road, San Jose, California 95120-6099,* and TETSUO KANAMOTO, *Science University of Tokyo, Department of Applied Chemistry, Kagurazaka, Shinzuku-ku, Tokyo 162, Japan*

Synopsis

A new morphological model is discussed which is based on the relation of tensile modulus and strength to the macrofibrillar dimensions (aspect ratio) and the shear modulus of ultrahigh molecular weight polyethylene fibrillar structures of draw ratio DR $\leq$ 200–300. Such structures were obtained by solid state deformation of the as-received powder and solution grown crystals using an extrusion-drawing process. According to this model, the highest tensile modulus and tensile strength values that can be obtained are 212 GPa and 13.3 GPa, i.e., significantly close to the theoretically calculated values.

INTRODUCTION

Many structural models have been proposed to explain the remarkable enhancement of the mechanical properties of deformed semicrystalline polymers under uniaxial flow conditions.[1-5] These models assume the development of crystal continuity or taut-tie molecules which connect crystallites longitudinally and provide an efficient load transmitting structural element, the load transfer occurring at a molecular level. For the most studied highly drawn polyethylene, many techniques have been used to determine the length and orientation distribution of the crystalline and amorphous chain extended components which unequivocally show that the remarkable tensile property enhancement depends strongly on the polymer chain extension achieved during processing. This conformational change has been described quantitatively by the molecular draw ratio, a quantity which allows the evaluation of the chain extension and, therefore, the efficiency of a molecular deformation process.[6,7] The conformational change, however, is meant to imply a change at a macroscopic level rather than at a molecular level since the latter includes areas of localized order, e.g., crystals, and disorder, e.g., amorphous phase. Traditionally, the degree of molecular anisotropy that results from a molecular deformation process has been evaluated by the determination of the crystalline and amorphous chain orientation and extension using complementary analytical techniques, including X-ray diffraction, birefringence, electron microscopy, Raman spectroscopy, and thermal analysis.[5,8-14] Recently, the small-angle neutron scattering technique has been used to determine quantitatively the changes in the molecular conformation and anisotropy of deformed

Journal of Applied Polymer Science, Vol. 35, 1265–1281 (1988)
 CCC 0021-8995/88/051265-17$04.00

polymers.[15-17] A thorough evaluation of these analytical techniques is discussed in a recent review by Porter et al.[18] The molecular draw ratio (MDR) has been emphasized only recently as an important parameter for the evaluation of the remarkable tensile property enhancement with draw, although various workers have discussed previously this quantity in relation to elastic recovery tests with drawn polymers in order to measure the degree of the residual chain extension. One of the reasons for ignoring the importance of the MDR in the evaluation of the tensile properties of drawn polymers arises from the fact that the characterization techniques give satisfactory correlations between the degree of crystalline and amorphous orientation and extension, and the mechanical properties enhancement in the "low draw ratio" range, DR $\leq$ 50, that we were capable of achieving until recently. However, in recent solid state deformation studies with solution grown ultrahigh molecular weight polyethylene (UHMWPE) crystal morphologies, such morphologies were deformed to fibrillar structures of DR ~ 200–300 which had a tensile modulus of ~ 220 GPa, i.e., in the range of the theoretically calculated values, and a tensile strength 4–5 GPa, i.e., only 0.3–0.25 of the theoretically calculated tensile strength values. In view of these recent developments, there are two important points that we should recognize:

(a) The spectacular increase of the tensile modulus with draw ratio is not accompanied with a similar increase in tensile strength when the polyethylene is superdrawn to DR $\geq$ 150.

(b) The superdrawn polyethylene fibrillar structures do not exhibit significantly different crystalline and amorphous extension and orientation values from the fibrillar structures which were obtained at DR < 50. This point becomes more complex when one considers that neither the upper limit of the crystalline chain extension nor the effect of the fraction of the amorphous phase (which decreases with DR) on the tensile property enhancement can be determined. Therefore, the question arises of whether the analytical approaches which are useful for measuring the degree of polymer chain extension provide an adequately measurable quantity which can relate the variation of the tensile properties with DR, and whether this quantity can be expressed in a way that will relate to some change at a molecular or morphological level.

In this report, we discuss the relation of the tensile properties to the DR of the fibrillar structures, obtained by drawing either UHMWPE solution grown crystals or the as-received powder stock, in terms of the aspect ratio of the macrofibrils of the drawn UHMWPE structures and their shear modulus, which varies significantly with DR. Furthermore, we propose a morphological model in which the structural unit is the macrofibril, that is, an entity composed of microfibrils with length of ~ 100 μm and diameter 1–10 μm, which allows the prediction of the maximum tensile properties that can be achieved for high density polyethylene by solid state deformation.

The proposed model is different from the previously proposed models by Peterlin,[4] Gibson et al.,[5] and Scott, and Clark[3] which are based on the crystalline deformation that occurs during the drawing process and in the way that the load is transferred within the highly oriented and extended semicrystalline structure at a molecular level. Peterlin suggests that the microfibril, an entity with length ~ 1 μm and diameter ~ 100 Å, is the fundamental

element for the high modulus performance. The microfibril consists of deformed crystalline lamellae connected by taut-tie molecules. Ward proposed that it is the crystalline continuity that gives rise to the high modulus. The crystalline continuity is ensured in the amorphous regions by the extended intercrystalline bridges which transmit the load from crystal to crystal. Clark suggested an extended chain crystalline structure to describe the high modulus performance with the chain folds and ends acting as defects in the crystalline structure. Barham and Arridge[19] have taken a different approach to describe the high modulus performance of the drawn morphologies. They proposed a short fiber composite model of needle-like crystals in a soft matrix in which the load is transferred from crystal to crystal through the soft matrix; the shear modulus of the matrix is assumed to remain constant during the different stages of the drawing process.

In our model, it is assumed that the crystalline deformation has occurred and the deformed crystals are connected by taut-tie molecules and/or intercrystalline connections (which ensure the crystalline continuity) that transfer the load within the microfibrillar and the macrofibrillar structures. The model attempts to explain how the load is transmitted at the macrofibrillar level, predict more realistically the modulus and strength property values that can be achieved by superdrawing, taking into consideration the variation of the tensile properties with DR over the draw ratio range 1–300, and explain the disparity between the theoretically predicted and the experimentally determined tensile property values.

RESULTS

This study is based on experimental data obtained with solid state deformed UHMWPE compacted powders of solution grown crystals, the as-received stock, as well as melt-crystallized morphologies, by extrusion and extrusion drawing to different draw ratios. Some physical and mechanical properties of solid state deformed UHMWPE from different initial morphologies are listed in Table I. The solution grown UHMWPE crystal aggregates

TABLE I
Physical and Mechanical Properties of Solid Deformed[a] UHMWPE from Different Initial Morphologies

UHMWPE	Draw ratio (max)	Melting point (°C)	Crystallinity (%)	Tensile modulus (GPa)	Tensile strength (GPa)	Strain at break (%)
Recrystallized morphology from $T > 220$°C	8	123	78	16	0.15	9
Compressed powder at 90°C	26	142	75	15	0.11	2
Compressed single crystal mats at 90°C	240	151	90–95	220	3.5–4	< 4

[a]Solid state deformation at 130°C.

with an average particle size ≤ 10 μm were compacted and deformed by extrusion followed by tensile drawing to a DR ~ 200–300.[20] Such superdrawn morphologies have a modulus of ~ 220 GPa and tensile strength ~ 4–5 GPa. In similar extrusion studies, the compacted powder of the as-received UHMWPE resin at 90°C (average powder particle size ~ 300 μm), which is known to have a chain folded crystalline morphology like the melt-crystallized morphologies, could be drawn only to a DR_{max} ~ 25. The value is lower by 1 order of magnitude than the DR_{max} (~ 250) achieved with the solution grown crystals, but it is significantly higher than the DR_{max} (≤ 8) obtained with the melt crystallized morphologies. The Young's modulus (~ 15 GPa) and tensile strength (~ 0.11 GPa) of the drawn products from the as-received resin are significantly lower than the respective properties of the drawn solution grown crystal morphologies but of the same order of magnitude with the properties of the drawn products from melt-crystallized morphologies. The overall deformability of the compacted powder morphologies below T_m can be explained by the absence of a molecular network (as is the case for the least drawable melt-crystallized morphology) between the powder particles which may deform into fibrils by interparticle friction; the dimensions of the fibrils depend on the extent of deformation. The solution grown crystalline morphologies can be drawn to a higher extent because of the smaller number of chain entanglements and inter- and intralamellar tie molecules in their more regular and adjacent reentry chain folded crystalline morphology.

The molecular draw ratio of the solid state drawn UHMWPE morphologies of different draw ratio was determined from elastic recovery tests, as described in Refs. 6 and 7. For example, the elastic recovery of an UHMWPE

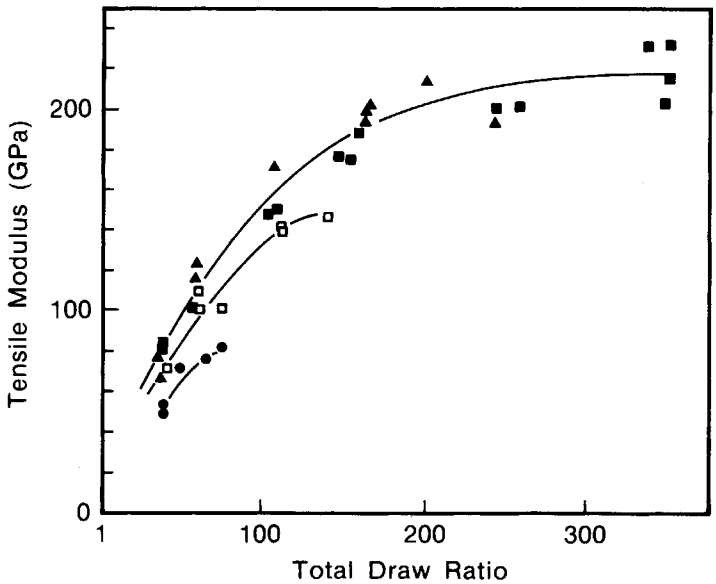

Fig. 1. Variation of the tensile modulus of superdrawn polyethylene crystalline morphologies of different molecular weight grown from solution with drawn ratio. MW($\times 10^{-5}$): (■) 21; (▲) 15; (□) 5; (●) 2.

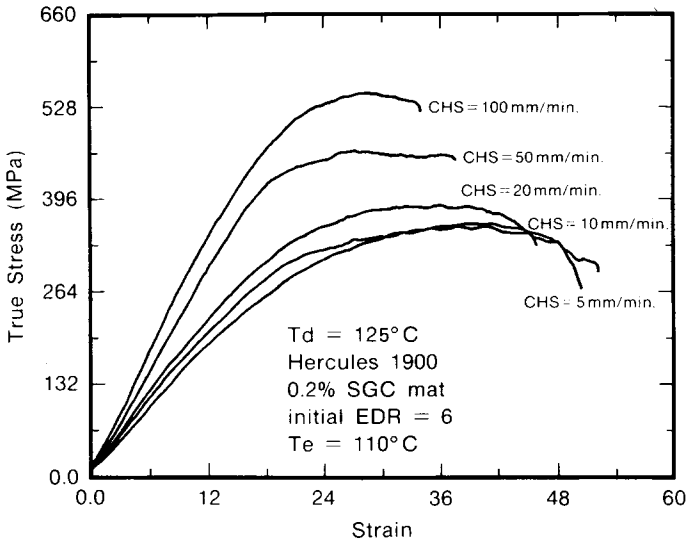

Fig. 2. Variation of the true stress for drawing at 125°C (T_d) and different cross head speeds (CHS) extrudates of UHMWPE solution grown crystals of extrusion drawn ratio (EDR) = 6. The extrudates were prepared at 110°C (T_e).

extrudate of DR = 25 obtained at 120°C from the as-received powder stock was 75%, whereas the elastic recovery of an extrudate of the same DR from a solution crystal morphology was 100%. The elastic recovery of a melt-crystallized UHMWPE morphology of DR ~ 8 (no higher DR could be obtained) was 100% also.

Furthermore, it is interesting to observe that for the superdrawn UHMWPE solution crystalline morphologies, the modulus varies linearly with DR up to 180 (Fig. 1). In the DR range 180–250, the modulus is less sensitive to DR, and, above DR ~ 250, it does not increase. A similar dependence of the modulus on DR is observed for the solution crystalline morphologies of a PE with M_w 2–15 × 10^5; however, the maximum DR that these resins could be drawn was significantly lower and depended on the M_w of the PE resin. As shown in Figure 2, the true draw stress increases with DR and approaches a constant value at DR ~ 150 that increases with the strain rate.

DISCUSSION

The results of our solid state extrusion and drawing studies of the compacted UHMPWE morphologies of solution grown crystals and the as-received powder stock are particularly suitable for the study of the proposed model because they provide a direct relation between the original average powder particle size and the dimension of the fibril at a given DR. Furthermore, with these morphologies, critical issues for the development of high modulus/strength properties such as the molecular continuity, the fraction of fibrils per cross-sectional area and the fraction of inter- and intrafibrillar taut molecular chains (subsequently referred to also as inter- or intrafibrillar connections) can be addressed.

Two important factors relating to the molecular continuity are the aspect ratio (AR) of the fibrils and the molecular weight. The former has always been discussed with respect to the sample dimensions. For example, Folkes and Arridge[21] have indicated that the St. Venant's principle does not hold for anisotropic samples such as the high modulus/strength fibrillar PE morphologies, and that an AR $\geq$ 80 is required in order to determine the modulus accurately. This argument can be considered also at the fibrillar level and is illustrated in the sequence of photographs in Figure 3. Since the load propagates preferentially along the surface of the fibril, it is obvious that a fibril of the same length but smaller diameter will transfer the load more uniformly and, therefore, effectively. Also, as the fibril is drawn to a higher DR, the contact area (overlap area) between adjacent fibrils increases. Directly related

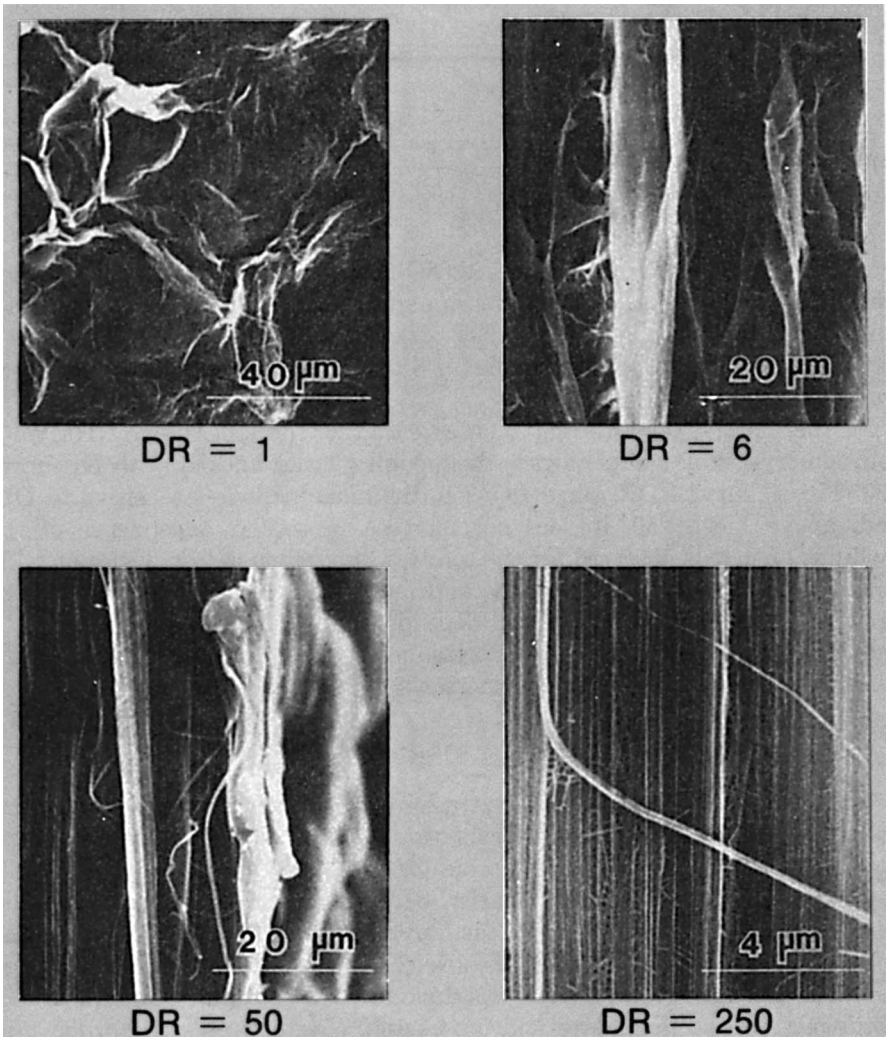

Fig. 3. Scanning electron micrographs of solution grown UHMWPE single crystal mats at different draw ratio.

to the longer fibril length are:

(a) the degree of molecular extension within the fibril and the fraction of intrafibrillar connections which affect mainly the modulus performance;
(b) the fraction of the interfibrillar connections which affects predominantly the strength performance.

Also important for attaining high modulus and strength performance by ultradrawing is the molecular weight of the polymer. The effect is best shown in the superdrawing of the solution grown crystalline polyethylene morphologies of different molecular weights (Fig. 1). In these morphologies, the deformation resistance is substantially decreased by the lower number of entanglements between molecular chains. The long chain nature of UHMWPE (up to 300,000 Å) inhibits relaxation and loss of molecular orientation and extension during the ultradrawing process and therefore provides a basis of molecular continuity within and between adjacent fibrils. The extent of molecular continuity relates to the molecular draw ratio and depends on the processing conditions and the initial morphology of the polymer.

In attempting to produce polymers with high modulus/strength, it is essential to pack as many chains, and therefore fibrils, per cross section as possible which in turn implies that it is essential to convert as effectively as possible the mechanical energy input into molecular chain orientation and extension. As shown in Table I, this can be achieved with a compacted powder by

(a) decreasing the average size of the powder particles which may transform at a given DR to smaller diameter fibrils, and therefore more fibrils/area in comparison to the number of fibrils/area that are formed from, e.g., a compacted powder morphology with $\gtrsim 10 \times$ larger powder particles (as received stock);
(b) making the initial morphology more deformable, e.g., solution grown vs. melt-crystallized morphology. These factors are both important for the development of high modulus and strength because they result in a larger number of effective load transmitter/area.

A simple way of viewing the deformation of a compacted powder is to consider the powder particle as a spherical particle (of diameter ~ 300 μm in the case of the as-received powder or ~ 10 μm for the solution crystalline morphology), which is deformed to an idealized cylinder, assuming constant volume. If the cylinder length to the sphere diameter equals the MDR, the diameter of the cylinder can be computed for a particular cylinder length $L = d_1 \cdot (\text{MDR})$ from

$$D = \sqrt{4V/L\pi} \tag{1}$$

where L = cylinder length, D = cylinder diameter, d_1 = sphere diameter, and V = volume of sphere; the aspect ratio of the cylinder, AR, can be determined from the ratio L/D. Thus the deformed compacted powder may be thought of

TABLE II
Variation of the Aspect Ratio of the Macrofibrils of Solid State Deformed UHMWPE Solution Grown Crystalline Morphologies at Different Temperatures with Their Molecular Draw Ratio (Calculated from Elastic Recovery Tests) and Tensile Properties

T	MDR	Tensile modulus (GPa)	Tensile strength (GPa)	Aspect ratio
25	6	5	—	18
24	21.5	40	0.5	122
25	42	72	0.5–1.0	333
60	64	99	1.0	628
60	132	161	2.5	1859
90	72	87	1.0	750
90	180	175	3.2–3.8	2950
115	60	115	0.5–1.0	1071
115	247	222	4.0–5.0	4750
130	66	102	0.5–1.0	653
130	120	160	2.0–2.5	1600
125[a]	18.2	15	0.1	57

[a]As-received powder stock.

as consisting of packed "macrofibrillar cylinders" of average size, that of the deformed cylindrical powder particle at a particular molecular draw ratio. The variation of the aspect ratio of the macrofibrils obtained by solid state deforming solution grown crystals of UHMWPE at different temperatures, with the associated MDR and tensile properties, is shown in Table II. The value of the morphologies drawn to DR_{max}, corresponding to MDR = 18.2 of the as-received UHMWPE powder stock, is included also. When the modulus and strength are plotted against the fibrillar dimensions (Fig. 4), i.e., the length and the diameter of the fibrils, the modulus increases monotonically with the fibrillar length and approaches a constant value in the very high DR region. The strength increases more rapidly with fibrillar length in the lower DR region and approaches a limiting value at a lower DR in comparison to the modulus. Both the modulus and strength increase rapidly as the fiber diameter decreases in the low draw ratio but are less sensitive to the fiber diameter decrease in the high draw ratio range.

The variation of the modulus of the drawn UHMWPE morphologies with the aspect ratio L/D of their macrofibrils in the drawn ratio range 1–300 can best be described by a plot of the log of the inverse modulus $1/E$ against the log of the $(L/D)^{-2}$ as shown in Figure 5. (The alternative notation $2 \log D/L$ is used for the $(L/D)^{-2}$ parameter.) A curve fitting equation to this plot is the logarithmic polynomial

$$\log(1/E) = A + B \log(x) + C \log(x)^2 \quad \text{for } 1 \leq DR < 300 \qquad (2)$$

where

$$x = (L/D)^{-2}$$

For high draw ratios, DR > 100, the variation of the inverse modulus, $1/E$,

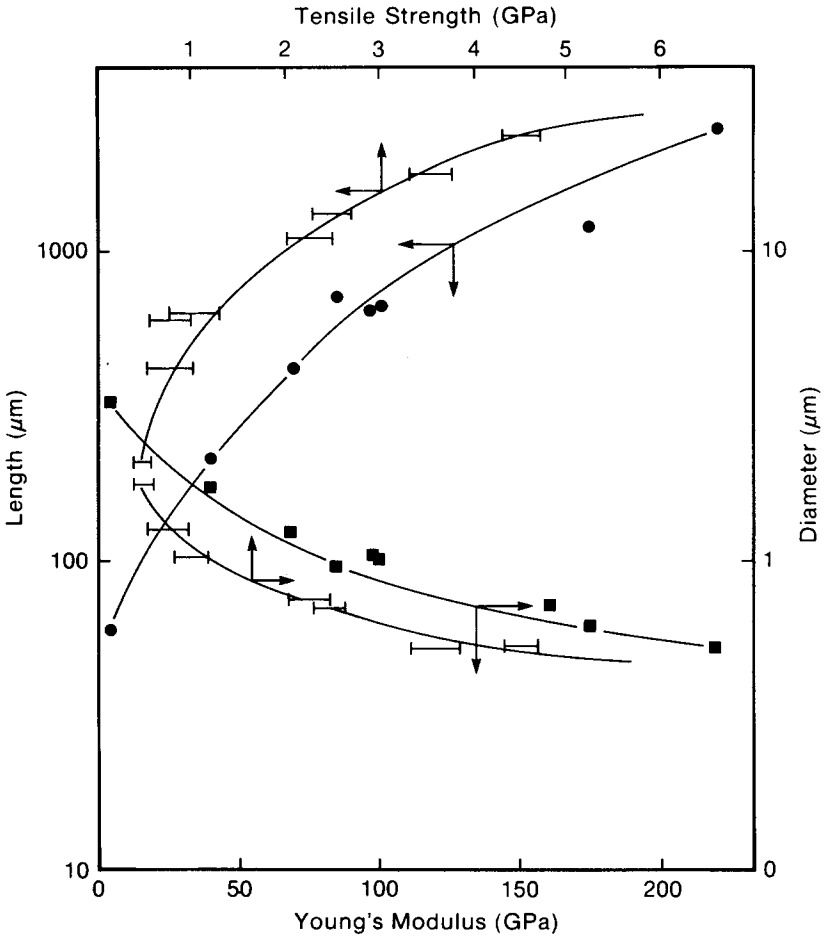

Fig. 4. Variation of the Young's modulus and tensile strength with the dimensions of the fibrils of drawn UHMWPE crystals grown from solution.

with $(L/D)^{-2}$, shown in Figure 6, is best described by the linear expression

$$\frac{1}{E} = \frac{1}{E_0} + M\left(\frac{L}{D}\right)^{-2} \quad \text{for DR} > 100 \tag{3}$$

where $1/E_0$ is the intercept at the $1/E$ axis and M is a constant. Least square analysis yields for this relation the numerical equation

$$\frac{1}{E} \times 10^3 = 4.72 + 0.454 \times 10^7\left(\frac{L}{D}\right)^{-2} \tag{4}$$

The modulus of the isotropic UHMWPE, i.e., at $L/D = 1$ can be obtained from the logarithmic plot in Figure 5, whereas the maximum modulus of a superdrawn fibrillar morphology can be obtained from the intercept, $1/E_0$, at the $1/E$ axis in Figure 6. For the UHMWPE, the calculated tensile modulus

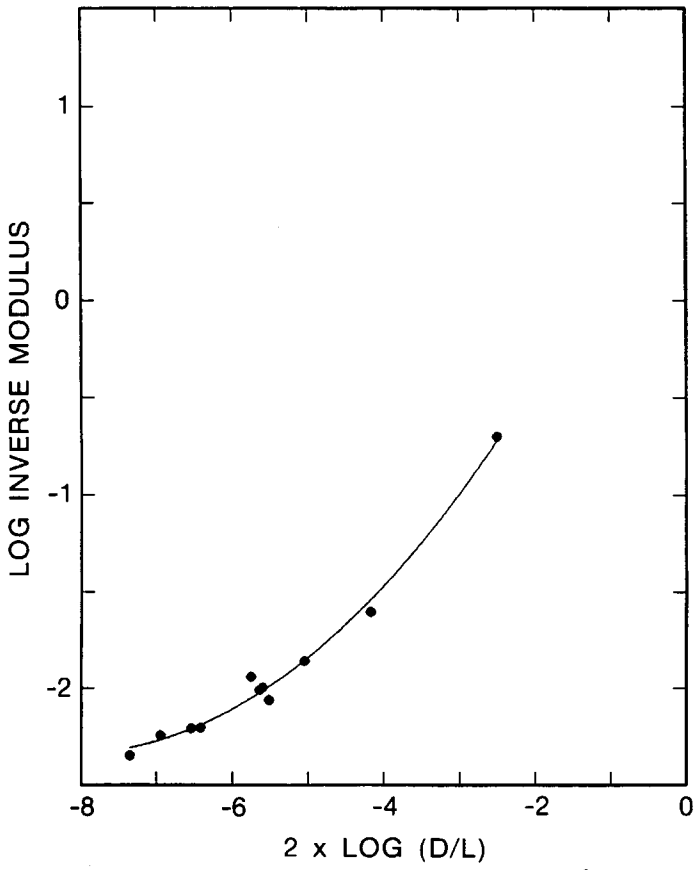

Fig. 5. Logarithmic plot of the inverse modulus against the $(L/D)^{-2}$ of the fibrils of drawn UHMWPE morphologies.

of the undrawn (isotropic) state is 0.089 GPa (actual limits $0.03 \leq E \leq 0.245$ GPa) and the maximum modulus that can be achieved by superdrawing is 212 GPa (actual limits $180 \leq E_0 \leq 272$).

Equation (3) is similar to the expression

$$\frac{1}{E_A} = \frac{1}{E_{\parallel}} + \frac{6}{5G} \cdot \left(\frac{l}{d}\right)^{-2}$$

describing the relation of the tensile modulus of a unidirectional glass fiber–epoxy composite[22] to the aspect ratio (l/d) of the tested sample where E_A is the apparent tensile modulus of the composite, $E_{\parallel}$ the tensile of the composite modulus, and G the shear modulus of the neat resin. This relation shows that the ability to transfer the load in the fiber direction is influenced by the tensile and shear properties of the composite. A fundamental difference between a unidirectional fiber–epoxy composite and a fibrillar morphology of a highly drawn UHMWPE is that the fibrils in the composite are embedded in an isotropic resin of some constant shear modulus value which provides all the lateral connectivity between adjacent fibrils, whereas in a highly drawn

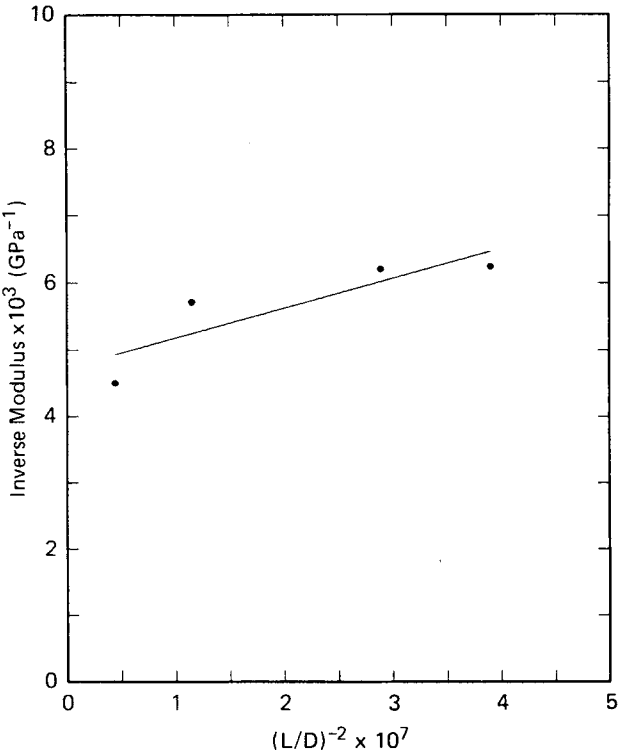

Fig. 6. Plot of the inverse modulus against the $(L/D)^{-2}$ of the fibrils of drawn UHMWPE morphologies at DR > 100.

fibrillar morphology the lateral connectivity is ensured by interfibrillar connections. However, the number of interfibrillar connections per unit fibrillar length between adjacent fibrils decreases as the DR increases. Thus, whereas a plot of the inverse tensile modulus against $(l/d)^{-2}$ for a unidirectional fiber–epoxy composite results in a straight line from the slope of which the shear modulus of the neat resin can be obtained, in the case of the highly drawn fibrillar morphology, this plot is nonlinear, presumably reflecting the shear modulus dependence on the DR which decreases gradually to a very low value as the DR becomes higher. It appears that the shear modulus varies considerably with DR for DR $\leq$ 100 and assumes a constant value in the high DR region, DR > 100, and hence the factor M in eq. (3), which includes the shear modulus contribution of the fibrillar structure, is constant at DR $\geq$ 100. The dependence of shear modulus on DR in the low DR region can be explained by the fact that during the transformation of the initial isotropic morphology to a fibrillar morphology, and, subsequently, the fibrils are held by fewer and fewer lateral interfibrillar connections per unit length as the DR increases, and eventually are held only by weak van der Waals forces in the lateral direction if one assumes that the drawing process may result eventually in a totally extended chain conformation. Thus, whereas the fibril length and consequently its surface area increases with DR, the shear modulus becomes extremely small irrespective of the fibrillar dimensions.

Since the number of the interfibrillar connections between adjacent fibrils relates directly to the shear modulus, the reduction of the interfibrillar connections per unit length with DR may be followed by the difference in the shear modulus values at a given DR that can be obtained using the numerical expression

$$\frac{1}{E} \times 10^3 = 4.72 + 0.454 \times 10^7 \left(\frac{L}{D}\right)^{-2} \tag{4}$$

of eq. (3),

$$\frac{1}{E} = \frac{1}{E_0} + M\left(\frac{L}{D}\right)^{-2} \tag{3}$$

in which the constant M includes the shear modulus G value (in the case of the unidirectional fiber-epoxy composite $M = 6/5G$), and the numerical form

$$\log \frac{1}{E} = 1.057 + 0.838 \log(x) + 0.0518[\log(x)]^2 \tag{5}$$

of eq. (2), where $x = (L/D)^{-2}$. The variation of the shear modulus with L/D or DR, which results in the nonlinear behavior in the plot of Figure 5, can be expressed by the equation

$$g = \frac{G(x)}{G_\infty} \tag{6}$$

where $x = L/D$ and G_∞ is the shear modulus value of the fibrillar morphology when $L/D \rightarrow \infty$; g can be calculated from the difference between eq. (3) and eq. (5), which can be expressed by

$$\Delta = \frac{1.2 \cdot x}{G_\infty}\left(1 - \frac{1}{g}\right) \tag{7}$$

The variation of g with L/D is shown by the logarithmic plot of G/G_∞ vs. x in Figure 7. From eqs. (4) and (7), $1.2/G_\infty = 4.54 \times 10^3$, and therefore the shear modulus of the superdrawn fibrillar morphology (for DR > 100) $G_\infty = 2.6 \times 10^{-4}$ GPa. The shear modulus of the polymer at DR = 1 or $L/D = 1$ is calculated to be 0.071 GPa, which is close to the shear modulus of HDPE (0.083 GPa).[23]

The fact that the modulus increases as the number of interfibrillar connections per unit length decreases shows that the modulus does not depend as much on the interfibrillar connections as it may depend on the intrafibrillar connections. In turn, this indicates that the modulus depends strongly on the fraction of fibrils per cross-sectional area. This is in agreement with the modulus and elastic recovery data of similarly drawn morphologies from the compacted as received and the single crystal morphologies powders shown in Table II. Despite the weak bonding between the deformed powder particles, the modulus of the drawn morphologies from the compacted as-received

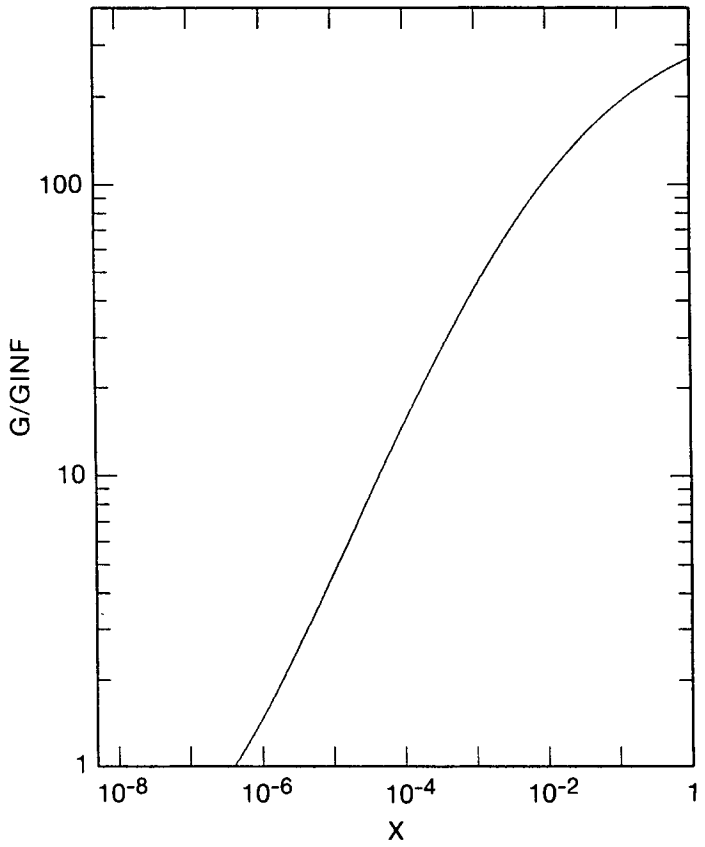

Fig. 7. Plot of the shear modulus variation with the L/D of the fibrils of drawn UHMWPE morphologies.

powders is ~ 10 × higher in comparison with the isotropic sample. Yet this modulus is only about 1/3 of the modulus of the similarly drawn solution grown crystalline morphology. Since both powders were compacted under the same pressure and temperature conditions, it may be assumed that it is the larger fraction of fibrils or the intrafibrillar connections rather than the lateral interfibrillar bonding per unit length that is most important for the high modulus performance. The number of intrafibrillar connections increases with DR or L/D, particularly in the low DR range (DR < 100), where a small shear displacement of microfibrils within the fibril can generate a large number of intrafibrillar connections. This is shown clearly in the sharp increase of modulus with the draw ratio in the low DR range (Fig. 1). Also, the elastic recovery data indicate that a much higher number of intrafibrillar connections is generated with the solution grown crystal morphology in comparison with the compacted as-received powder, in which the powder particles are deformed with significant amount of interparticle slippage (as is suggested by their lower elastic recovery ~ 75%).

So far, we have discussed the modulus dependence on the fibrillar dimensions and the molecular continuity within and between the fibrils in a fibrillar

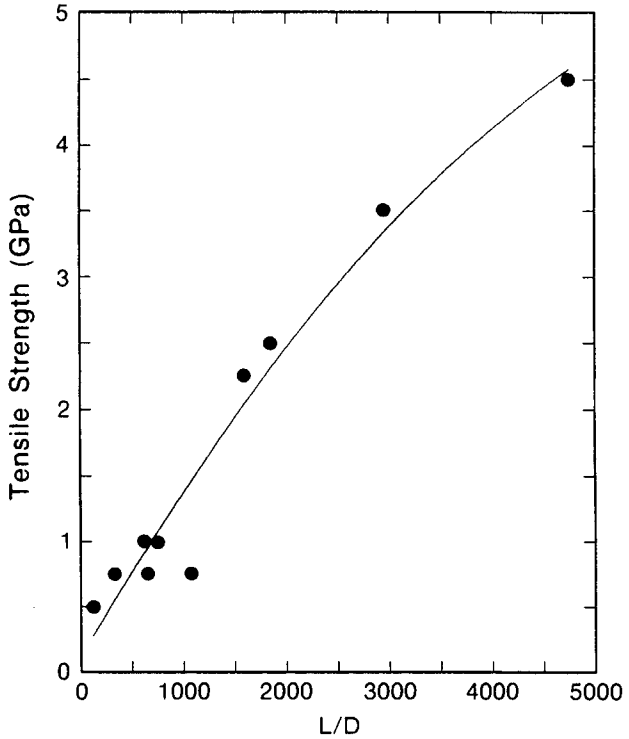

Fig. 8. Plot of the tensile strength against the L/D of the fibrils of drawn UHMWPE morphologies.

morphology. It is clear that fibrillar morphologies with modulus values very close to the theoretically predicted values can be obtained, and that the length of the fibrils and the degree of molecular organization within the fibrils is very important for the achievement of the ultrahigh modulus values. What is the tensile strength dependence on these parameters particularly in view of the fact that the maximum tensile strength ever determined is only 1/3 to 1/4 of the theoretical strength (15–18 GPa). As shown in Figure 8, the tensile strength increases with L/D or DR until it reaches a maximum value (for UHMWPE) at ~ 5 GPa. These data when replotted on a logarithmic scale as inverse strength vs. $(L/D)^{-2}$ (Fig. 9) are best described by the equation

$$\log \frac{1}{S} = K + N \log(x) \tag{8}$$

where $x = (L/D)^{-2}$, $K = -0.331$, and $N = 0.323$. Since the strength and the modulus show a similar dependence on the fibril diameter (Fig. 4), but the strength reaches a limiting value with length, it is clear that the strength depends strongly on the number of interfibrillar connections per unit length, which, of course, decreases with increasing L/D or DR, and, therefore, a limiting value for the tensile strength much lower than the theoretically calculated values is expected. The maximum tensile strength value of a superdrawn fibrillar morphology can be calculated from an inverse strength,

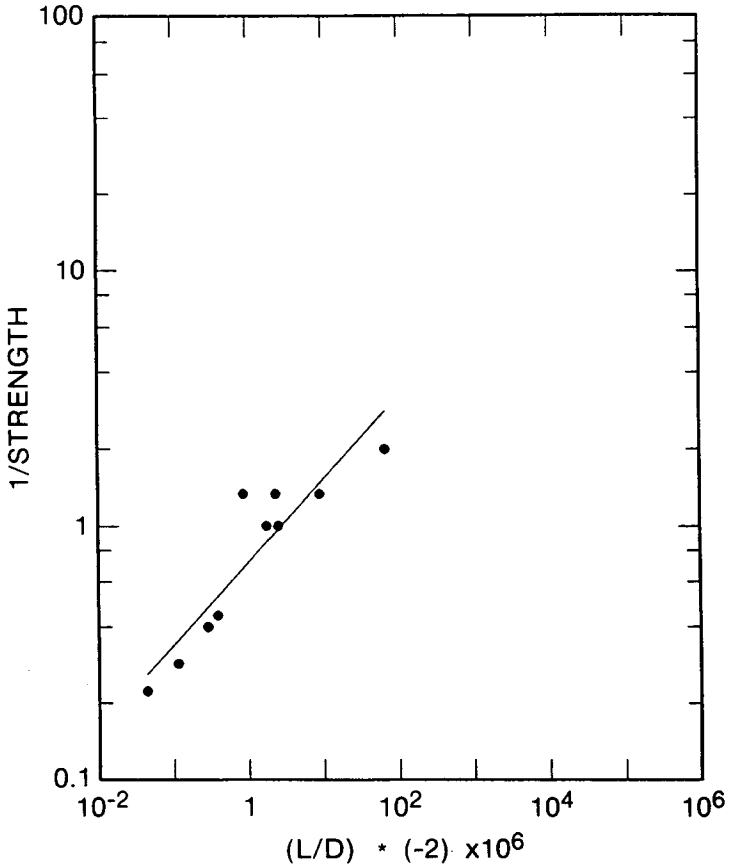

Fig. 9. Logarithmic plot of the inverse tensile strength against the $(L/D)^{-2}$ of the fibrils of drawn UHMWPE morphologies.

$1/S$, vs. $(L/D)^{-2}$ plot for L/D values for draw ratios about 100. Such a plot, shown in Figure 10, is best described like the $1/E$ vs. $(L/D)^{-2}$ plot, by the linear relation

$$\frac{1}{S} = \frac{1}{S_0} + Q\left(\frac{L}{D}\right)^{-2} \quad \text{for DR} > 100 \tag{9}$$

where $1/S_0$ is the intercept of the $1/S$ axis and Q is a constant. Least square analysis yields for this relation the numerical equation

$$\frac{1}{S} = 0.0075 + 1.35 \times 10^6\left(\frac{L}{D}\right)^{-2} \tag{10}$$

Thus the maximum tensile strength at $L/D \rightarrow \infty$ is calculated to be 13.3 GPa. The significant difference between the theoretically predicted strength values and the present extrapolated value based on the experimental data presumably reflects the marked difference in the fracture mechanisms taken into consideration. The former was calculated by assuming chain rupture

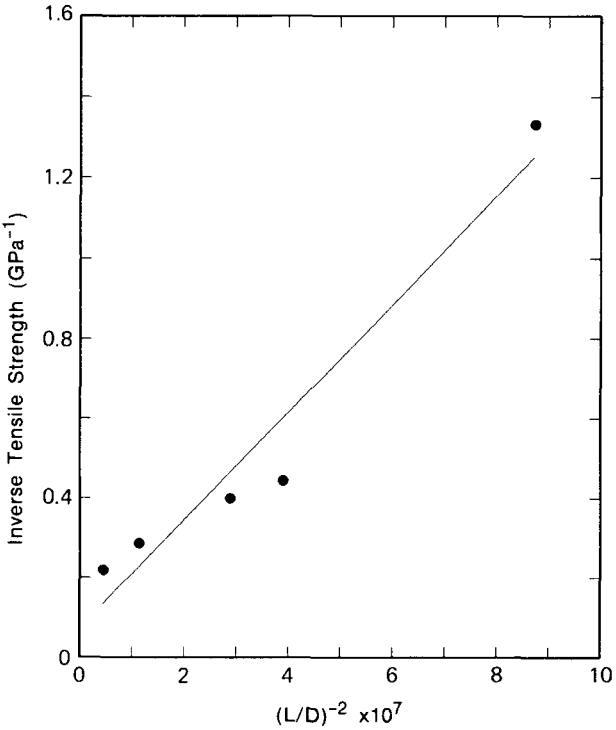

Fig. 10. Plot of the inverse tensile strength against the $(L/D)^{-2}$ of the fibrils of drawn UHMWPE morphologies at DR > 100.

whereas the actual sample failure in tension occurs with extensive fibrillation, indicating that the fracture propagates along the fibrillar interfaces.

The dependence of tensile strength on the number of interfibrillar connections is illustrated with the variation of the true draw stress with strain in Figure 2. The true stress increases with strain but remains unchanged with increasing strain from 25 to 35%, corresponding range of DR, 150–210, where-after it decreases as the strain increases further. This behavior must associate with the decreasing number of interfibrillar connections rather than the failure of intrafibrillar connections because, concurrently, the modulus increases with DR up to DR ~ 250 and then remains unchanged. The deformation at this point presumably involves excessive shear displacement of poorly bonded fibrils in the lateral direction which leads to crack formation and eventually catastrophic failure. The effect of poor interfibrillar bonding on the tensile strength has been shown with the extruded UHMWPE samples of DR ~ 25 from the compacted as-received powder which have very low tensile strength (~ 0.11 GPa) and elongation to break (2%) in comparison with melt-crystallized morphologies of UHMWPE that were drawn to a significantly lower DR (DR ~ 8) but had comparable modulus and strength values.

CONCLUSION

The results of this study suggest that the tensile properties of ultradrawn UHMWPE can be related to the macrofibrillar dimension changes and the

shear modulus of its fibrillar morphology at a particular drawn ratio. Whereas the Young's modulus is sensitive to the fraction of the intrafibrillar connections which increase with draw ratio, the tensile strength shows a stronger dependence on the number of the interfibrillar connections per unit length of the macrofibrils which decrease as the draw ratio increases. On the basis of the ultradrawing studies of the compacted powders of ultrahigh molecular weight polyethylene morphologies, a model was proposed according to which the highest Young's modulus and tensile strength values that can be obtained are 212 GPa and 13.3 GPa, i.e., significantly close to the theoretically calculated values.

The authors wish to thank Dr. T. Karis for his assistance in the computational analysis.

References

1. A Cifferi and I. M. Ward, Eds., *Ultra High Modulus Polymers*, Applied Science, London, 1975.
2. M. Takayanagi, K. Imada, and T. Kagiyama, *J. Polym. Sci., Part C*, **15**, 263 (1966).
3. E. S. Clark and L. S. Scott, *Polym. Eng. Sci.*, **14**, 682 (1974).
4. A. Peterlin, *J. Mater. Sci.*, **6**, 490 (1971).
5. A. G. Gibson, G. R. Davies, and I. M. Ward, *Polymer*, **19**, 683 (1978).
6. M. P. C. Watts, A. E. Zachariades, and R. S. Porter, *J. Mater. Sci.*, **15**, 426 (1980).
7. R. S. Porter, M. Daniels, M. P. C. Watts, J. R. C. Pereira, S. J. DeTeresa, and A. E. Zachariades, *J. Mater. Sci.*, **16**, 1134 (1981).
8. A. Peterlin and R. Corneliussen, *J. Polym. Sci., A-2*, **6**, 1273 (1968).
9. T. Kanamoto, S. Fujimatsu, A. Tsuruta, K. Tanaka, and R. S. Porter, *Rep. Prog. Polym. Phys. Jpn.*, **24**, 185 (1981).
10. E. S. Sherman, R. S. Porter, and E. L. Thomas, *Polymer*, **23**, 1069 (1982).
11. R. G. Snyder, S. J. Kruse, and J. R. Scherer, *J. Polym. Sci., Polym. Phys. Ed.*, **16**, 1593 (1978).
12. A. Peterlin and R. G. Snyder, *J. Polym. Sci., Polym. Phys. Ed.*, **19**, 1727 (1981).
13. G. Capaccio, I. M. Ward, and M. A. Wilding, *J. Polym. Sci., Polym. Phys. Ed.*, **19**, 1489 (1981).
14. Y. K. Wang, D. A. Waldman, R. S. Stein, and S. L. Hsu, *J. Appl. Phys.*, **53**, 6591 (1982).
15. J. S. Higgins and R. S. Stein, *J. Appl. Crystallog.*, **11**, 346 (1978).
16. G. Hadziioannou, L. H. Wang, R. S. Stein, and R. S. Porter, *Macromolecules*, **15**, 880 (1982).
17. D. M. Sadler and J. A. Odell, *Polymer*, **21**, 479 (1980).
18. R. S. Porter, H. H. Chuah, and T. Kanamoto, to appear.
19. P. J. Barham and R. G. C. Arridge, *J. Polym. Sci., Polym. Phys. Ed.*, **15**, 1177 (1977).
20. T. Kanamoto, A. Tsumita, K. Tanaka, M. Taheda, and R. S. Porter, *Polym. J.*, **15**, 327 (1983).
21. M. J. Folkes and R. G. C. Arridge, *J. Phys. D*, **8**, 1053 (1975).
22. A. Golovoy and H. van Oene, Proc. of SPE RETEC on High Performance Engineering Materials, October 16–17, 1984, Mississauga, ON, Canada.
23. J. M. C. Cowie, *Polymers: Chemistry and Physics of Modern Materials*, International Textbook Company Limited, Aylesbury, Bucks, Great Britain, 1973.

Received June 20, 1987
Accepted July 22, 1987